Available online at www.sciencedirect.com
SCIENCE DIRECT®
Journal of Nuclear Materials 337–339 (2005) 1038–1042
journal of nuclear materials
www.elsevier.com/locate/jnucmat

Divertor impurity sources; effects of hot surfaces and thin films on impurity production

M.F. Stamp [a,*], P. Andrew [a], S. Brezinsek [b], A. Huber [b], JET EFDA Contributors [1]

[a] EURATOM/UKAEA Fusion Association, Culham Science Centre, Abingdon, Oxon, OX14 3DB, UK
[b] Institut für Plasmaphysik, Forschungszentrum Jülich GmbH, EURATOM-Association, D-52425 Jülich, Trilateral Euregio Cluster, Germany

Abstract

Strong continuum emission has been observed from divertor tiles at visible wavelengths and identified as Planck radiation from surfaces with temperatures of typically ~2600 K. Such hot spots (which are not tile edges) can persist for several seconds and are more common at the inner divertor, than the outer. Surprisingly, these hot spots do not usually produce significant impurity fluxes. In contrast, ELMs may produce a significant enhancement of impurity fluxes, depending on strike point location and ELM size.

PACS: 52.40.Hf; 52.25.Rv; 52.55.Fa; 52.25.Vy
Keywords: Impurity sources; Thermography; Divertor; Carbon impurities; JET

1. Introduction

Graphite is widely used in present-day tokamaks and is proposed as part of the ITER divertor [1]. It has good power handling properties, but off-normal events such as disruptions or giant ELMs that lead to carbon sublimation ($T > 3000$ K) are predicted to severely limit the divertor lifetime [2]. At lower surface temperatures (e.g. 2500 K), the gross erosion rate of the graphite tiles will be reduced, but a higher Z_{eff} may result in unacceptable fuel dilution. This study examines the consequences of overheated graphite (CFC) tiles in the JET divertor.

2. Method

Spectrometers and interference filter–photomultiplier tube combinations are used to monitor bremsstrahlung emission at 523.5 nm (±0.5 nm), in order to calculate the plasma Z_{eff}. However, if hot tiles are present in the same line-of-sight (l-o-s), then Planck radiation will also be detected. The variation of Planck emission with temperature means that in JET, the Planck emission at 523.5 nm is equal to the visible bremsstrahlung emission for surface temperatures of ~1900 K. Additionally, since the spectrometers are used with a 50 ms integration

* Corresponding author. Tel.: +44 1235 464989; fax: +44 1235 464535.
E-mail address: mike.stamp@jet.uk (M.F. Stamp).
[1] Annex of J. Pamela et al., Fusion Energy 2002, Proc. 19th IAEA Fusion Energy Conf., Lyon, 2002.

0022-3115/$ - see front matter © 2004 Elsevier B.V. All rights reserved.
doi:10.1016/j.jnucmat.2004.07.061

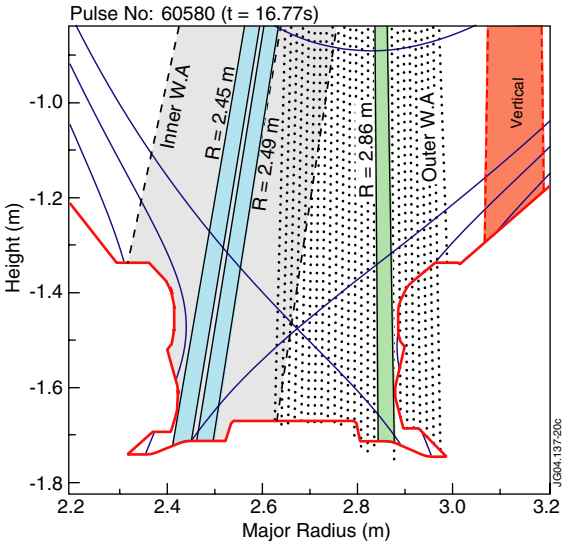

Fig. 1. Single optical fibres collect light from the diagnostic lines-of-sight (l-o-s) indicated; 2 wide-angle divertor l-o-s, 3 high resolution (33 mm diameter) l-o-s and the vertical l-o-s.

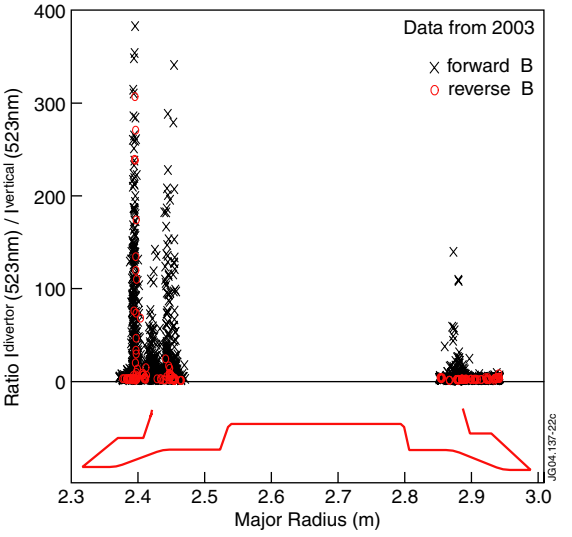

Fig. 2. MkII SRP data for the 523.5 nm enhancement versus strike point position. Each data point is from a different discharge. Some data was from operation with reversed magnetic field, B.

time, emission from short-lived hot spots ($t < 1$ ms, e.g. from ELMs) may not be distinguishable from intrinsic molecular and bremsstrahlung emission: a 1 ms duration hot spot at 2600 K will emit the same 523 nm Planck radiation as a 50 ms hot spot at 1900 K.

The central physics file (CPF) database was used to identify the existence and location of hot spots on JET tiles, using these 523.5 nm l-o-s signals. The vertical l-o-s is on a chord that passes close to the plasma centre onto a carbon tile outside the divertor. This tile receives no significant power loading during a discharge. Consequently, the ratio of the divertor to the vertical signal is sensitive to the Planck radiation in the divertor l-o-s and has been used to identify hot spots. This ratio typically has a value of 2–6, but when a hot spot is in the l-o-s, the ratio can reach values of >100.

Fig. 1 shows the geometry of the l-o-s used in this work. The two wide-angle l-o-s are useful for detecting the existence of hot spots, while the narrower l-o-s provide some spatial information on the hot spots.

3. Results

3.1. Location and frequency of hot spots

Fig. 2 shows a plot of the 523 nm emission ratios for the MkII SRP divertor. The emission ratio is plotted as a function of the strike point location, for all discharges with the strike points on the horizontal target plates. In 2003, there were 1931 discharges with the inner strike point on the horizontal targets and 373 of these exhibited hot spots (defined as a 523 nm emission ratio >20). Of the 1592 discharges with the outer strike point on the horizontal target, only 21 had hot spots. A similar number of discharges were run with the strike points on the vertical target tiles (these are not plotted in Fig. 2), but the 523 nm emission ratio was always less than 50 and only >20 for 11 (0) discharges with the strike point on the inner (outer) vertical target tiles.

The figure illustrates that hot spots occur predominantly at the inner divertor and on the horizontal tile close to the pumping slot in the divertor corner. The outer divertor hot spots, though less common, are also located on a horizontal tile close to the pumping slot in the divertor corner. These hot spot locations have been identified as areas of redeposition [3]. No difference can be seen between operation with forward or reversed magnetic field.

Similar results are found for MkII SRP data from 2002. In this case, 6 of the 24 outer divertor hot spots, at $R = 2.88$ m, were in consecutive discharges and probably resulted from the heating of a temporary redeposition zone: for these discharges, #56975–56980, the strike point history [4] seems to be an important factor, since 11 out of the previous 13 discharges had the outer strike point on the horizontal target at $R = 2.853$ or 2.871 m, that is, at shorter major radius than the hot spot. (A simple erosion model would predict erosion at the strike point and deposition in the scrape-off layer).

Data from 2000 for the MkII GB divertor also show a similar pattern to Fig. 2. There were 250 hot spots from 733 discharges with strike points on the inner

horizontal tile and 4 hot spots from 616 discharges with strike points on the outer horizontal tile.

The appearance of hot spots is attributed by Andrew et al. [5] to the heating of surface films, sometimes with only modest input power (see Fig. 5, later), that are in poor thermal contact with the underlying divertor tile.

3.2. Temperature measurements

The JET survey spectrometer (420–600 nm) records sufficient wavelength range that the shape of the continuum emission versus wavelength can be used to derive an 'average' Planck temperature of the hot spot. The spectrometer has an integration time of 50 ms and a l-o-s spatial resolution of 33 mm, so the measurements are a weighted average over time and space. We find that the spectral data is fitted well by assuming a single Planck temperature for the hot spot (e.g. see Fig. 3).

Fig. 3 shows three frames of data from this spectrometer, each 100 ms apart. Thermal temperatures (T^{vis}) of up to 2650 K are derived from the wavelength dependence of the emission. Though the emission in Fig. 3(c) is 4 × larger than in Fig. 3(b), implying a ΔT of 350 K, the measured temperature is only 130 K higher – implying a change in the emission area. Indeed, comparing the absolute divertor emission with a Planck body, then the effective emission area (at the measured temperature) increases from 9% to 21% of the area in the l-o-s (33 mm diameter spot). This implies that the

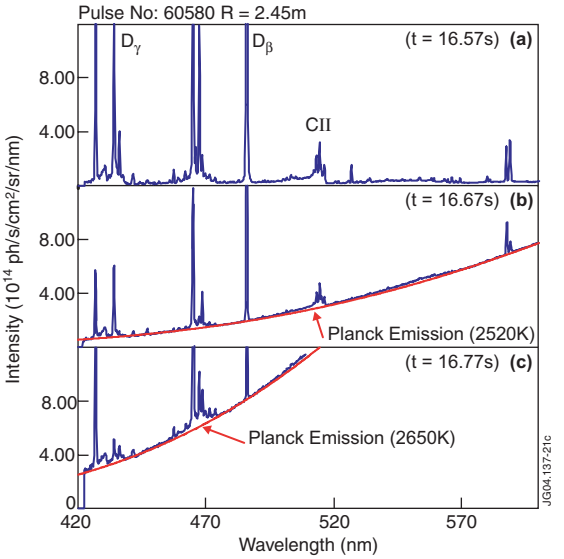

Fig. 3. Calibrated spectra for the inner divertor l-o-s at $R = 2.45$ m. (a) A 'normal' spectrum at a time ($t = 16.57$ s) before the hot spot. (b) Spectrum 100 ms later ($t = 16.67$ s, $T^{vis} \sim 2520$ K). (c) Spectrum another 100 ms later ($t = 16.77$ s, $T^{vis} \sim 2650$ K).

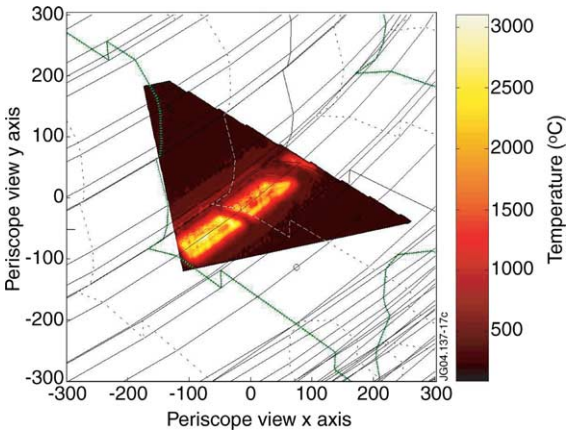

Fig. 4. IR camera image ($t = 16.65$ s), showing peak temperature of ~2800 K. The hot spot is clearly broad and non-uniform. The solid green line indicates the divertor cross-section (cf. Fig. 1).

'hot spot' is not a uniform hot layer, but is granular (dust or carbon grains or CFC high-points), consistent with similar observations by Herrmann [6]. There is IR camera data for this discharge, Fig. 4, which shows a broad hotspot at the inner divertor, in agreement with other visible spectroscopy that shows equal Planck emission on the two narrow inner divertor l-o-s at $R = 2.45$ and 2.49 m (Fig. 1). Since the visible and IR measurements sample different portions of the Planck emission curve, yet give the same thermal temperature, these

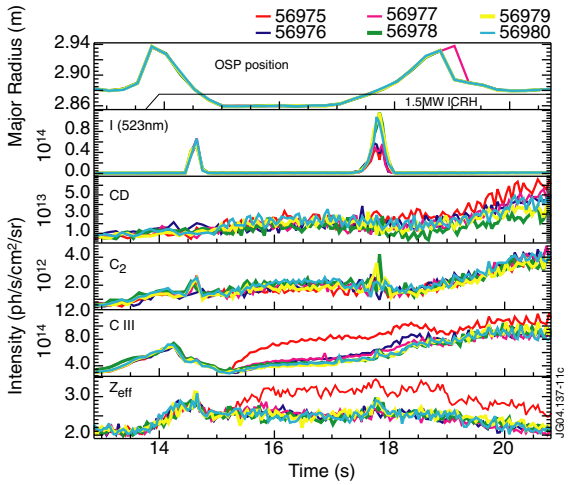

Fig. 5. Outer strike point (OSP) position and spectroscopy data for the swept strike point discharges, #56975–80. The intensity of emission at 523 nm, $I(523)$, is a measure of the hot spot temperature. The first discharge had a lower density and consequently a higher Z_{eff}.

measurements rule out strong molecular emission (at μm wavelengths) as an explanation of previous anomalous IR observations [5].

The centre divertor tile, the septum replacement plate (SRP) tile, in the MkII SRP divertor was observed (at visible wavelengths) to reach high temperatures only twice, in discharges #54823 ($T^{vis} \sim 2800$ K, for the tile edge at $R = 2.80$ m) and #61248 ($T^{vis} \sim 2780$ K). #54823 was a discharge to assess the SRP power handling, whilst for #61248 the outer strike point was accidentally too low. The SRP tile was not designed for power loading, unlike all the other divertor target tiles, which were engineered so that tile edges are always hidden from the plasma.

3.3. Consequences of hot spots

During an L-mode experiment that required a slow sweep (17–23 s) of the strike points from the horizontal tiles onto the vertical tiles to a height of −1.5 m (see Fig. 1), a hot spot was created in the outer divertor at $R = 2.88$ m, $t = 14.65$ and 17.83 s (Fig. 5). The first hot spot occurs as the strike point moves across $R = 2.88$ m in preparation for the later slow sweep. The Planck emission from this hot spot was very reproducible (first 3 and last 3 pulses had different gas fuelling, which seems to change the time evolution of the second hot spot), indicating that the high temperatures ($T^{vis} \sim 2600$ K from visible emission; no IR data available) were not modifying the surface conditions (i.e. not removing any films). Fig. 5 also illustrates that the hot spot has only a minor influence on the carbon impurity influxes and Z_{eff} ($\Delta Z_{eff} \leqslant 0.2$).

At the inner divertor, where there is significant redeposition of eroded first wall material [3], hot spots are regularly detected (Section 3.1). One example, with high power heating (20 MW) and a fixed strike point position is shown in Fig. 6. The Planck emission is high during most of the heating phase, though it does drop significantly around 12 s, indicating a reduced temperature at this time. The measured temperatures at 10.0 s are $T^{IR} \sim 2075$ K; $T^{vis} \sim 2350$ K. The difference is most likely due to the toroidal averaging in the IR camera analysis, though toroidal asymmetries between the locations of the IR and visible diagnostics are also possible.

The correlation in the early time evolution (8–10 s) of the signals in Fig. 6 suggests that there is some thermal release of carbon impurities. However, from 10 s onwards, there is no correlation of the carbon impurity emission with the Planck emission. This may indicate that carbon dust, or 'soft' amorphous films, are quickly eroded in the first seconds, to leave a more resilient 'conditioned' surface.

Although most data indicates that these hot spots do not generate significant impurities, there are exceptions, for example, #60580, when $T^{IR} \sim 2800$ K (Fig. 4) and increases in Z_{eff}, due to enhanced carbon fluxes, were observed.

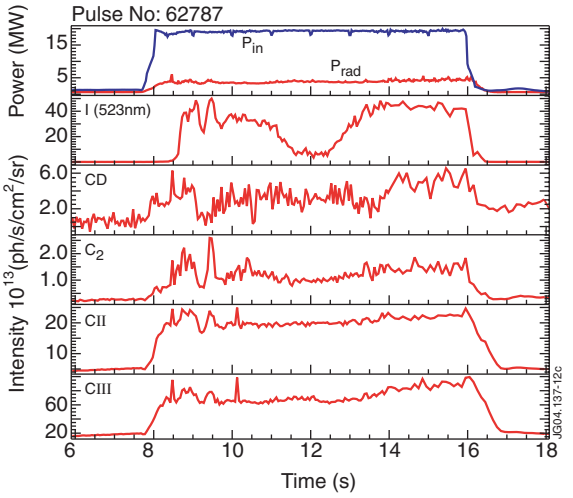

Fig. 6. Input power, radiated power and spectroscopy data for the fixed strike point discharge, #62787. The intensity of emission at 523 nm, $I(523)$, is a measure of the hot spot temperature.

3.4. ELM power loading

ELMs have the potential for extreme heating of divertor target tiles: MJ of plasma energy can be incident on the tiles in 0.1–1 ms. The ITER requirement is that the ELM power loading must be less than about 1 MJ/m^2 [2]. Although visible spectroscopy is unlikely to see the Planck emission produced by short-lived ELMs, as explained earlier, the 40 μs time resolution of the JET IR camera system is capable of capturing such fast events.

Fig. 7(a) and (b) show inner divertor spectra for a horizontal target ELM-ing discharge in JET, with 0.5MJ ELMs. Planck radiation during ELMs is not evident from the spectra, as expected from the IR camera measurement of $T^{IR} \sim 1900$ K. However, these ELMs generate large influxes of CII and C_2. The ELM-averaged CII and CIII carbon fluxes (assuming constant photon efficiency) are increased by ~50%.

Fig. 7(c)–(e) show similar data for another discharge with 1.0 MJ ELMs (i.e. ~1 MJ/m^2). In this case the strike points were on the vertical target tiles. The spectra look quite different; although there are large increases in CII and CIII, the increases in C_2 are smaller (and variable, cf. Fig. 7(d) and Fig. 7(e)) and many metal lines (Be, Cr) can be observed. Some spectra show a small amount of Planck emission, but the intensity is too low to distinguish it from molecular and bremsstrahlung emission and derive a thermal temperature. The IR

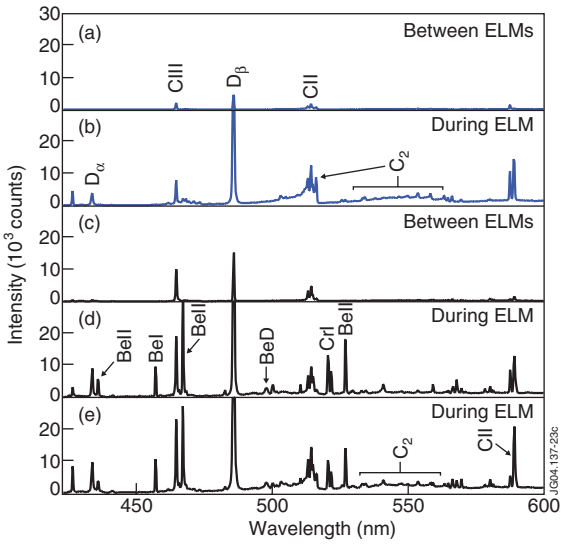

Fig. 7. Survey spectrometer data from discharges #60580 (a,b) and #62218 (c)–(e). (b) Shows enhanced molecular emission during an ELM (at $t = 13.37$ s). (d) and (e) Show strong Be and Cr emission (and variable C_2 emission) during ELMs at $t = 19.52$ s and $t = 19.77$ s, respectively.

camera measures $T^{IR} = 2500$–2800 K, so the surface is much hotter than in the previous case. During the ELMs, Z_{eff} is observed to ratchet upwards (for a total ΔZ_{eff} of 1.0), so core contamination has also risen.

4. Summary

Hot spots with temperatures >2400 K have been observed in the JET divertor with visible spectroscopy diagnostics. Hot spot locations and temperatures correlate well with the IR camera diagnostic, ruling out long wavelength molecular emission as a consideration in the interpretation of the IR camera signals.

Hot spots are found to be most common in the inner divertor and often last several seconds at typical temperatures ~2600 K. They are located on the horizontal target plates (not tile edges) in the divertor corners, on regions identified as areas of material redeposition. The hot spots may extend up to 6 cm poloidally and seem to have a granular structure – they are not a uniformly hot film. This may be due to the CFC surface structure, or soot/dust particles on the surface. Typically, these hot spots do not generate significant extra impurity, though when temperatures rise to 2800 K (where thermal sublimation should become important), increases in carbon fluxes and Z_{eff} are observed.

On shorter timescales (~0.1 ms), ELMs may cause hot spots that are not detectable with the JET visible spectrometers. If the ELMs fall onto deposition regions, fluxes of molecular carbon (C_2) can be significantly enhanced – likely due to thermal decomposition of amorphous carbon films. If large ELMs (1MJ) impact the metal-rich vertical target tiles, C_2 emission is not so pronounced, but carbon, beryllium and chromium atom/ion emission is significantly increased. The threshold for thermal ablation of the CFC tiles is expected to be at about this ELM size.

We have demonstrated the first use of an absolutely calibrated survey spectrometer (420–600 nm) to measure both the surface temperature (from the intensity variation of the Planck emission with wavelength) and the temperature homogeneity (from the measured emission intensity versus the expected emission at the measured temperature) of hot spots on divertor CFC tiles.

Acknowledgments

This work has been conducted under the European Fusion Development Agreement and is partly funded by EURATOM and the United Kingdom Engineering and Physical Sciences Research Council.

References

[1] G. Federici, J.N. Brooks, D.P. Coster, et al., J. Nucl. Mater. 290–293 (2001) 260.
[2] G. Federici, A. Loarte, G. Strohmayer, PPCF 45 (2003) 1523.
[3] J.P. Coad, P. Andrew, D.E. Hole, et al., J. Nucl. Mater. 313–316 (2003) 419.
[4] H.G. Esser, V. Philipps, M. Freisinger, et al., these Proceedings. doi:10.1016/j.jnucmat.2004.10.112.
[5] P. Andrew, J.P. Coad, T. Eich, et al., J. Nucl. Mater. 313–316 (2003) 135.
[6] A. Herrmann, et al. 10th Carbon Workshop 2003.